

The amplitude of mass density fluctuations at $z \approx 3.25$ from the Ly α forest of Q1422+231

Adi Nusser¹ and Martin Haehnelt²

¹ *Physics Department, The Technion-Israel Institute of Technology*

² *Max-Planck-Institut für Astrophysik, Karl-Schwarzschild-Str. 1, 85740 Garching*

1 June 2021

ABSTRACT

The real-space optical depth distribution along the line of sight to the QSO Q1422+231 is recovered from two HIRES spectra using a modified version of the inversion method proposed by Nusser & Haehnelt (1999). The first two moments of the truncated optical depth distribution are used to constrain the density fluctuation amplitude of the intergalactic medium (IGM) assuming that the IGM is photoionized by a metagalactic UV background and obeys a temperature-density relation. The fluctuation amplitude and the power law index α of the relation between gas and neutral hydrogen (H I) density are degenerate. The *rms* of the IGM density at $z \approx 3.25$ estimated from the first spectrum is $\sigma = \sqrt{\exp[(1.8 \pm 0.27)^2/\alpha^2] - 1}$, with $1.56 < \alpha < 2$ for plausible reionization histories. This corresponds to $0.9 \lesssim \sigma \lesssim 2.1$ with $\sigma(\alpha = 1.7) = 1.44 \pm 0.3$. The values obtained from the second spectrum are higher by $\approx 20\%$. If the IGM density traces the dark matter (DM) as suggested by numerical simulations we have measured the fluctuation amplitude of the DM density at an effective Jeans scale of about a hundred to two hundred (comoving) kpc. For CDM-like power spectra the amplitude of dark matter fluctuations on these small scales depends on the cosmological density parameter Ω . For power spectra normalized to reproduce the space density of present-day clusters and with a slope parameter of $\Gamma = 0.21$ consistent with the observed galaxy power spectrum, the inferred Ω can be expressed as: $\Omega = 0.61 (\alpha/1.7)^{1.3} (x_J/0.62)^{-0.6}$ for a flat universe, and $\Omega = 0.91 (\alpha/1.7)^{1.3} (x_J/0.62)^{-0.7}$ for a $\lambda = 0$ universe. x_J is the effective Jeans scale in (comoving) $h^{-1}\text{Mpc}$. Based on a suit of detailed mock spectra the $1\text{-}\sigma$ error is $\approx 25\%$. The estimates increase with increasing Γ . For the second spectrum we obtain 15% lower values.

Key words: cosmology: theory, observation, dark matter, large-scale structure of the Universe — intergalactic medium — quasars: absorption lines

1 INTRODUCTION

The Lyman forest in QSO absorption spectra is now generally believed to be caused by absorption by large-scale H I density fluctuations of moderate amplitude in a warm photo-ionized intergalactic medium (IGM). This is substantially different from the old cloud picture for the Ly α forest (see Rauch 1998 for a review). It is mainly sustained by cosmological hydrodynamical simulations which successfully reproduce the absorption features in QSO spectra (Cen et al. 1994; Petitjean, Mückel & Kates 1995; Zhang, Anninos & Norman 1995; Hernquist et al. 1996; Miralda-Escudé et al. 1996, Theuns et al. 1998). The picture had, however, been suggested before these numerical simulations became available (Bond, Szalay & Silk 1988; Bi, Börner & Chu 1992). Important results of the simulations are a tight correlation between the H I and the dark matter distribution (on scales larger than the Jeans length of the IGM) and a simple gas temperature-density relation which depends only on the reionization history of the Universe (Hui & Gnedin 1997, Haehnelt & Steinmetz 1998). As a consequence, the Ly α forest can be an important probe for the distribution of dark matter and its evolution over a wide redshift range (c.f. Weinberg 1999 for a review) on scales smaller than those accessible by the galaxy distribution or the lensing effects of foreground large scale structures on background galaxies (c.f. Bartelmann & Schneider 1999).

For example, Gnedin & Hui (1998) showed that the column density distribution of Ly α absorption lines depends on the

amplitude of the density fluctuations in the IGM. Croft et al used the flux power spectrum of QSO absorption spectra to constrain the DM power spectrum on scales from $2h^{-1}$ to $12h^{-1}$ Mpc (Croft et al. 1998, Croft et al. 1999, Weinberg et al. 1999). Nusser and Haehnelt (1999) (hereafter NH99) proposed an iterative procedure to obtain the real space density and its probability distribution function. Here we apply a modified version of this technique to two HIRES spectra of the QSO Q1422+231. We infer the fluctuation amplitude of the DM density on the effective Jeans scale and constrain the normalization constant of the optical depth distribution which depends on the ionization rate Γ_{phot} , the baryon density Ω_{bar} and the Hubble constant ($\mathcal{A} \propto \Omega_{\text{bar}}^2 h^3 / \Gamma_{\text{phot}}$). Section 2 describes our modified technique to extract moments of the probability distribution (PDF) of the density and presents tests on mock spectra. In section 3 we present the application to the data. Section 4 discusses implications for the cosmological density parameter. In section 5 we relate our work to previous work and give an outlook. Section 6 contains our conclusions.

2 THEORETICAL BACKGROUND

2.1 Basic equations

The optical depth in redshift space due to resonant Ly α scattering is related to the HI density along the line of sight (LOS) in real space by

$$\tau(w) = \sigma_0 \frac{c}{H(z)} \int_{-\infty}^{\infty} n_{\text{HI}}(x) \mathcal{H}[w - x - v_{\text{p}}(x), b(x)] dx, \quad (1)$$

where σ_0 is the effective cross section for resonant line scattering, $H(z)$ is the Hubble constant at redshift z , x is the real space coordinate (in km s^{-1}), \mathcal{H} is the Voigt profile normalized such that $\int \mathcal{H} dx = 1$, $v_{\text{p}}(x)$ is the LOS peculiar velocity, and $b(x)$ is the Doppler parameter due to thermal/turbulent broadening. The absorption features in the Ly α forest are mainly produced by regions of moderate densities where photoheating is the dominant heating source and shock heating is not important. Hydrogen in the IGM is highly ionized (Gunn & Peterson 1965, Scheuer 1965) and the photoionization equilibrium in the expanding IGM establishes a tight correlation between neutral and total hydrogen density. This relation can be approximated by a power law $n_{\text{HI}} \propto n_{\text{H}}^{\alpha}$, where the parameter α depends on the reionization history. The possible range for α is $1.56 \lesssim \alpha \lesssim 2$ with a value close to 2 just after reionization, and decreasing at later times (Hui & Gnedin 1997). Numerical simulations have shown that the gas density traces the fluctuations of the DM density on scales larger than the Jeans length, so that $n_{\text{HI}} = \hat{n}_{\text{HI}} \left(\frac{\rho_{\text{DM}}(\mathbf{x})}{\bar{\rho}_{\text{DM}}} \right)^{\alpha}$, where \hat{n}_{HI} is the HI density at mean dark matter density. In this relation $\rho_{\text{DM}}(\mathbf{x})$ is the dark matter density smoothed on the Jeans length scale below which thermal pressure becomes important. The Jeans length in the linear regime is given by (comoving),

$$\begin{aligned} x_{\text{J,lin}} &= \frac{2\pi c_s}{\sqrt{4\pi G \bar{\rho}}} (1+z) \\ &\approx 1.3 \left(\frac{\Omega h^2}{0.125} \right)^{-1/2} \left(\frac{\hat{T}}{1.5 \times 10^4 \text{ K}} \right)^{1/2} \left(\frac{1.5}{1 + (2 - \alpha)/0.7} \right)^{1/2} \left(\frac{1+z}{4} \right)^{-1/2} \text{ Mpc}, \end{aligned} \quad (2)$$

where c_s is the sound speed. However, in the non-linear regime gas can collapse to scales smaller than this and the Jeans scale becomes a somewhat ambiguous quantity. Here we define an effective non-linear Jeans length, x_{J} , as the width of a kernel of the form $[1 + (kx_{\text{J}}/2\pi)^2]^{-2}$, such that the rms fluctuation amplitude of $\rho_{\text{DM}}(\mathbf{x})$ is the same as that of the unsmoothed dark matter density filtered with this kernel (see section 4 for details). On scales larger than the effective Jeans length, equation (1) can be written as

$$\tau(w) = \mathcal{A}(z) \int_{-\infty}^{\infty} \left(\frac{\rho_{\text{DM}}(\mathbf{x})}{\bar{\rho}_{\text{DM}}} \right)^{\alpha} \mathcal{H}[w - x - v_{\text{p}}(x), b(x)] dx, \quad (3)$$

with

$$\begin{aligned} \mathcal{A}(z) &= \sigma_0 \frac{c}{H(z)} \hat{n}_{\text{HI}} \\ &\approx 0.61 \left(\frac{300 \text{ km s}^{-1} \text{ Mpc}^{-1}}{H(z)} \right) \left(\frac{\Omega_{\text{bar}} h^2}{0.02} \right)^2 \left(\frac{\Gamma_{\text{phot}}}{10^{-12} \text{ s}^{-1}} \right)^{-1} \left(\frac{\hat{T}}{1.5 \times 10^4 \text{ K}} \right)^{-0.7} \left(\frac{1+z}{4} \right)^6, \end{aligned} \quad (4)$$

where Ω_{bar} is the baryonic density in terms of the critical density and Γ_{phot} is the photoionization rate per hydrogen atom. The Doppler parameter in the last equation depends on n_{HI} as $b \propto n_{\text{HI}}^{1-\alpha/2}$.

NH99 have presented a direct Lucy-type iterative scheme to recover the optical depth and the corresponding mass and velocity fields in the LOS from the normalized flux, $F = \exp(-\tau)$. They showed that the density field can be successfully recovered below a threshold value above which the corresponding flux saturates. NH99 further used mock spectra extracted

from an N-body simulation to show that the moments of the mass density can be reasonably well estimated by fitting a log-normal PDF to the low density tail of the PDF of the recovered density. In the next section we present a modified method for estimating the moments of the density distribution.

2.2 Moments of the density PDF from the recovered local optical depth

NH99 provided an estimate for the quantity

$$\tilde{\tau}(x) \equiv \mathcal{A} \left[\frac{\rho(x)}{\bar{\rho}} \right]^\alpha, \quad (5)$$

which we term the local optical depth. It is related to the observed optical depth τ by a convolution with a Voigt profile as described in equation (1). The recovered $\tilde{\tau}$ is a good approximation to the true field only in regions with $\tilde{\tau}$ less than a certain value. For large optical depths, the recovered $\tilde{\tau}$ typically underestimates the true field. We define a truncated local optical depth $\tilde{\tau}_t$ as $\tilde{\tau}_t = \tilde{\tau}$ for $\tilde{\tau} < \tilde{\tau}_c$, and $\tilde{\tau}_t = 0$ otherwise. The corresponding truncated moments of $\tilde{\tau}_t$ can be written in terms of the density PDF as,

$$\langle \tilde{\tau}_t^n \rangle = \mathcal{A}^n \int_{-\infty}^{\delta_c} (1 + \delta)^{n\alpha} P(\delta) d\delta, \quad (6)$$

where $\delta = \rho/\bar{\rho} - 1$ is the density contrast and $\delta_c = (\tilde{\tau}_c/\mathcal{A})^{1/\alpha} - 1$. We further define $\nu = [\ln(\rho/\bar{\rho}) - \mu_1]/\mu_2$, where μ_1 and μ_2 are the average and *rms* values of $\ln(1 + \delta)$. NH99 had also shown that the PDF of the DM density smoothed on the scale relevant for the Ly α forest (the effective Jeans scale) can be reasonably well approximated by a log-normal distribution (Bi & Davidsen 1997, cf. Sheth 1998 and Gaztanaga & Croft 1998 for different forms of the PDF). For a log-normal density distribution, $P(\nu) = \exp(-\nu^2/2)/\sqrt{2\pi}$, the truncated moments in (6) can be written as,

$$\langle \tilde{\tau}_t^n \rangle = \frac{\mathcal{A}^n}{2} \exp\left(\frac{1}{2}n^2\alpha^2\mu_2^2 + n\alpha\mu_1\right) \left[1 + \operatorname{erf}\left(\frac{\nu_c - n\alpha\mu_2}{\sqrt{2}}\right)\right] \quad (7)$$

where ν_c is the value of ν corresponding to δ_c . By expressing ν in terms of $\tilde{\tau}$ in (7) we find

$$\langle \tilde{\tau}_t^n \rangle = \frac{1}{2} \exp\left(\frac{1}{2}n^2\alpha^2\mu_2^2 - n\alpha\mu_2^2/2 + n \ln \mathcal{A}\right) \left[1 + \operatorname{erf}\left(\frac{\ln \tilde{\tau}_c - n\alpha^2\mu_2^2 - \ln \mathcal{A} + \alpha\mu_2^2/2}{\alpha\mu_2\sqrt{2}}\right)\right]. \quad (8)$$

We have here used the relation $\mu_1 = -\mu_2^2/2$ which follows from the condition $\langle \delta \rangle = 0$ for the log-normal. The moments of the truncated optical depth distribution depend on four parameters \mathcal{A} , μ_2 , α and $\tilde{\tau}_c$. The parameter $\tilde{\tau}_c$ is chosen such that for $\tilde{\tau} < \tilde{\tau}_c$ the local optical depth does not suffer from the biases introduced in saturated regions. As apparent from equation (10) there are two basic degeneracies leaving us with two independent parameters:

$$\mathcal{B} \equiv \ln \mathcal{A} - \alpha\mu_2^2/2, \quad \mathcal{C} \equiv \alpha\mu_2. \quad (9)$$

In terms of these two parameters, the moments of $\tilde{\tau}_t$ can finally be written as

$$\langle \tilde{\tau}_t^n \rangle = \frac{1}{2} \exp\left(\frac{1}{2}n^2\mathcal{C}^2 + n\mathcal{B}\right) \left[1 + \operatorname{erf}\left(\frac{\ln \tilde{\tau}_c - n\mathcal{C}^2 - \mathcal{B}}{\sqrt{2}\mathcal{C}}\right)\right]. \quad (10)$$

The first two moments, $\langle \tilde{\tau}_t \rangle$ and $\langle \tilde{\tau}_t^2 \rangle$, are therefore sufficient to determine the parameters \mathcal{B} and \mathcal{C} . From these we can then infer the *rms* fluctuation amplitude of the DM density and the normalization constant of the optical depth \mathcal{A} as discussed in section 3.3. The use of truncated moments of the local optical depth has a number of advantages. It is numerically more stable than fitting a parametric form of the PDF to the distribution of the recovered density. It allows to introduce a cut-off in the form of an optical depth instead of the density which depends on the a priori unknown value of \mathcal{A} . Finally, it shows the basic degeneracies between α , μ_2 and \mathcal{A} .

In reality the PDF of the mass density smoothed on an effective Jeans scale is expected to be somewhat more positively skewed than a log-normal. The relations derived above can easily be generalized to other forms of the density PDF. We were, however, not able to constrain the additional skewness parameter of an Edgeworth expansion. The same was found by NH99. We therefore used a log-normal PDF for the analysis of the data. We assess the possible biases that arise in the determination of \mathcal{C} and \mathcal{B} using mock spectra in the next section.

3 APPLICATION TO THE SPECTRUM OF Q1422+231

3.1 The data

We had two spectra of Q1422+231 at $z = 3.62$ available for our analysis. The spectra were observed with the HIRES spectrograph by Rauch et. al. (1997) and Songaila & Cowie (1996) on the Keck I telescope. The resolution of the spectra is

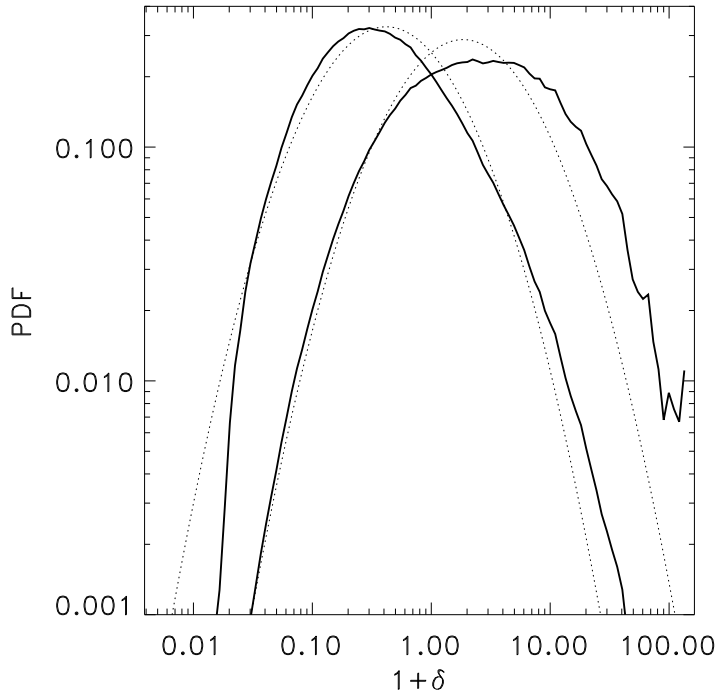


Figure 1. The curves on the right are the PDFs of $\ln(1 + \delta)$ for an Edgeworth expansion around a log-normal distribution with $\mu_3 = 0.4$. The curves on the left show $(1 + \delta)P[\ln(1 + \delta)]$. The solid curves are the average of 70 PDFs from which the mock spectra of Q1422 were generated. The dotted lines correspond to a log-normal PDF with the same value of μ_2 .

$\approx 8 \text{ km s}^{-1}$ and the pixel size is 2.5 km s^{-1} . We used the wavelength region from 4742 \AA ($\text{Ly}\beta$ at the redshift of the QSO) to 5618 \AA ($\text{Ly}\alpha$ at the redshift of the QSO) to avoid confusion due to an overlap of intervening $\text{Ly}\alpha$ and $\text{Ly}\beta$ absorption. This corresponds to a redshift range from $z = 2.9$ to $z = 3.62$ and is equivalent to $240h^{-1} \text{ Mpc}$ (comoving) in an Einstein-de Sitter Universe. The two spectra were continuum-fitted independently by the observational groups. The differences in our results should thus give an idea of the error due to continuum-fitting.

3.2 Error estimates and tests of the procedure using mock spectra

Two sources of errors are important for our analysis: first the intrinsic error caused by the inversion procedure; second the cosmic variance error resulting from the use of only one quasar spectrum with limited redshift range. We quantify these errors and possible systematic biases by analyzing mock spectra. The mock spectra were produced using a modified version of the method suggested by Bi et al. (1992) [see also Bi & Davidsen (1997)]. The mock spectra have the same redshift range, pixel size, resolution and S/N as the observed spectra of Q1422. We generated random realizations of a Gaussian density field with a linear CDM-like power spectrum. We then assumed a parametric form for the PDF of the non-linear density and obtained the non-linear density field along the LOS from the linear field by a rank-ordered mapping (Weinberg 1992). The corresponding non-linear peculiar velocity, v_{pec} , was computed as described in NH99. The optical depth was calculated using equation (3) with $\alpha = 1.7$ and $b = 16n_{\text{HI}}^{0.15} \text{ km s}^{-1}$. The factor \mathcal{A} was chosen such that the mean flux decrement in the mock spectrum matches the observed value. Finally, instrumental broadening as well as photon and pixel (read out) noise was added.

Based on numerical simulations, we expect the true PDF to be more positively skewed than a log-normal. Our method for estimating \mathcal{B} and \mathcal{C} assumes, however, that the PDF is log-normal. It is therefore important to test the sensitivity of the estimated moments to the shape of the true PDF. We generated mock spectra for a log-normal and for PDFs described by an Edgeworth expansion around the log-normal,

$$P(\nu) = (2\pi)^{-1/2} \exp(-\nu^2/2) \left[1 + \frac{\mu_2\mu_3}{3!} (\nu^3 - 3\nu) \right], \quad (11)$$

where the skewness parameter is defined as $\mu_3 = \langle \nu^3 \rangle / \mu_2$. N-body simulations with Gaussian initial conditions have shown this parameter to be positive, independent of the detailed shape of the initial power spectrum (Colombi 1993, NH99). We will present detailed results for two different PDFs with $(\mu_2, \mu_3 = 1.3, 0.0)$ and $(1.0, 0.4)$, but we have also tested the technique with $(0.9, 0.6)$. In figure 1 we show representations of the PDF with $\mu_3 = 0.4$. The deviations of the PDF of $(1 + \delta)$ from a

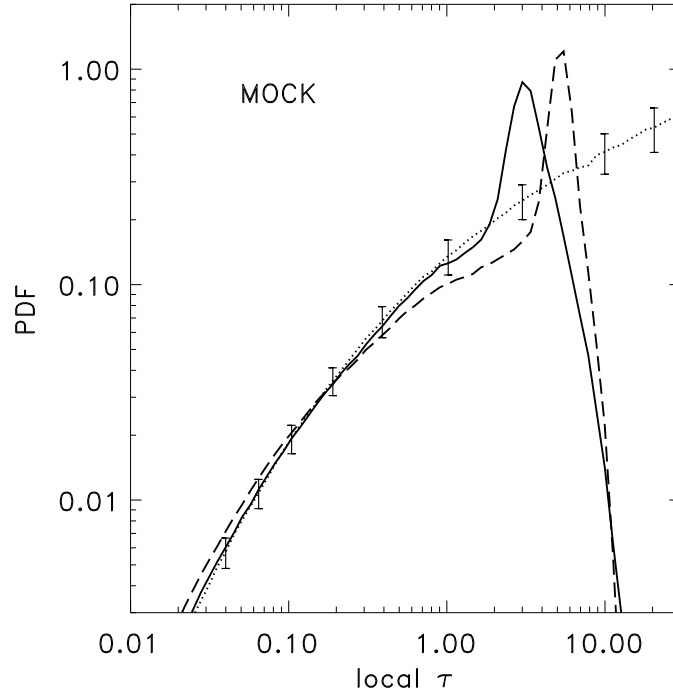


Figure 2. Curves of $\tilde{\tau}P[\ln(\tilde{\tau})]$ for the recovered and true local optical depth for mock spectra generated with $\mu_3 = 0.4$. The solid and dashed curves are for the recovered $\tilde{\tau}$ in real and in redshift space. The dotted line correspond to the mean of the true PDFs of the 70 mock spectra. The error bars represent the cosmic variance error (*rms* values of the deviations of the mock spectra from the mean PDF).

log-normal distribution with the same μ_2 are significant only for $\delta \gtrsim 2$. Since only the low density part of the PDF is relevant for the truncated moments, the method is expected to produce reasonable estimates of μ_2 even if the true PDF is somewhat skewed relative to log-normal. We have generated mock spectra for both PDFs with and without peculiar velocities to test the effect of redshift distortions. For each case 70 mock spectra (i.e. 70 random realizations for the same density power spectrum) were analyzed.

We have also modified the inversion procedure by introducing a power law relation between the Doppler parameter and the local optical depth, $b = b_0 \tilde{\tau}^{1-\alpha/2}$. This has significantly speeded up the convergence of the inversion. To determine b_0 we define the function $\chi^2 = \sum_{\text{pixels}} (F_i^{\text{obs}} - F_i^{\text{rec}})^2 / \sigma_i^2$, where σ_i is the error and F_i^{obs} the observed flux in pixel i . F_i^{rec} is the flux which corresponds the recovered local optical depth. We choose b_0 to be the largest value which gives $\chi^2/\text{pixel} = 1$ after a certain number of iterations.

In Fig. 2 the average $\tilde{\tau}P[\ln(\tilde{\tau})]$ of the recovered local optical depth of 70 mock spectra is shown (for the case with $\mu_3 = 0.4$) in real (solid curve) and redshift space (dashed curve). The dotted line represents the average true PDF. The error bars are 1σ cosmic variance errors calculated from the 70 random realizations. The spikes in the PDFs of the recovered local optical depth are due to the systematic underestimate in saturated regions. Figure 2 demonstrates that we have successfully corrected for redshift distortions in regions of low optical depths. This correction shifts the location of the prominent spike to lower $\tilde{\tau}$ because the redshift distortions tend to enhance the real space density contrast. We use the location of the spike to choose the cut-off $\tilde{\tau}_c$ for the truncated moments.

We have calculated the first two moments $\langle \tilde{\tau} \rangle$ and $\langle \tilde{\tau}^2 \rangle$ for three cutoff values, $\tilde{\tau}_c = 1.0, 1.5$ and 2.0 . The parameters \mathcal{B} and \mathcal{C} were determined by solving equations (10) with Broyden's method (e.g. Press et al 1992). Figures (3) and (4) show the true *vs* the recovered values of the parameters \mathcal{B} and \mathcal{C} for four sets of 70 mock spectra (two input PDFs, with and without peculiar velocities).

The tight correlation between the true and recovered values demonstrates robustness of the method. The estimated values of \mathcal{C} are unbiased in all four cases while \mathcal{B} is systematically underestimated (except in the log-normal case with peculiar velocities set to zero). We found similar results for the mock spectra produced with ($\mu_2 = 0.9, \mu_3 = 0.6$)

In tables (1) and (2) we list the mean values of $(\mathcal{C}, \mathcal{B})$ and the estimated errors determined from the four sets of 70 mock spectra. The intrinsic random error introduced in the inversion method is the *rms* value of the differences between estimated and true values from each set of the 70 realisations. The cosmic variance errors are estimated as the *rms* values of the true parameters. For both the skewed and the log-normal PDFs the estimated and true values of \mathcal{C} agree well within the 1σ errors.

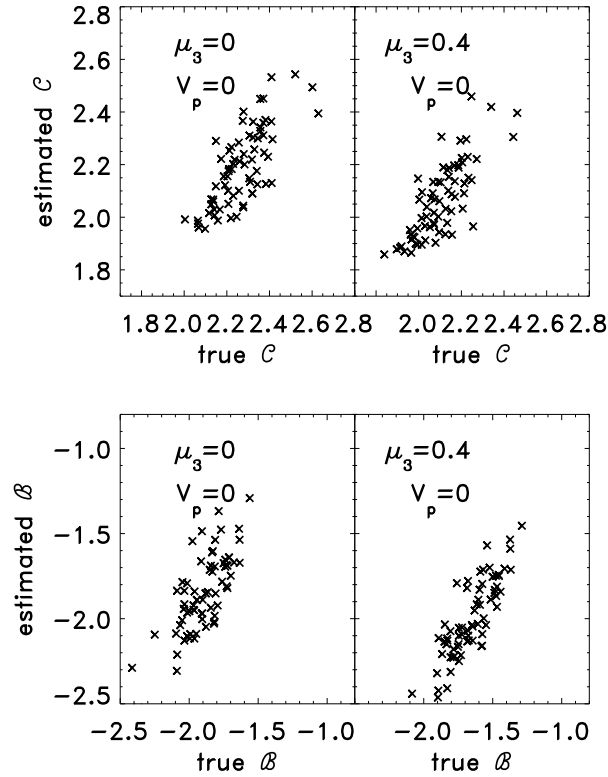


Figure 3. The estimated vs true C and B for 70 different random realizations of mock spectra generated with $v_{\text{pec}} = 0$.

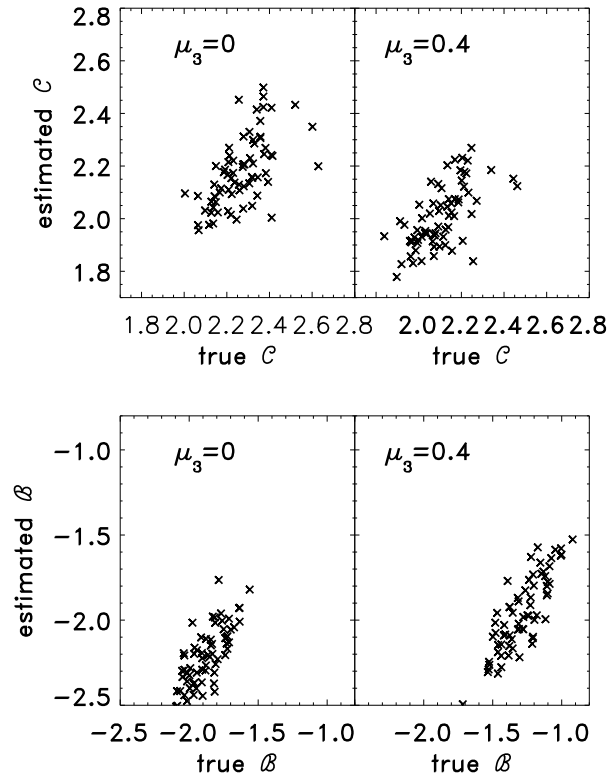


Figure 4. The same as the previous figure but for spectra generated with non-vanishing peculiar velocities.

Table 1. True and estimated parameters for the mock q1422+231 spectra generated with a log-normal PDF of the mass density. Listed are estimated parameters from mock spectra with and without peculiar velocities ($v_{\text{pec}} = 0$). The first entry shows the parameters estimated after correcting for redshift distortions, the second before the correction and the third the parameters from spectra generated with $v_{\text{pec}} = 0$. The first and second rows are $(\mathcal{C}, \mathcal{B})$ and the 1σ error due to the inversion. The fourth entry lists the true values of the parameters and the 1σ error due to cosmic variance. The transformation from \mathcal{C} and \mathcal{B} to \mathcal{A} is given by $\ln \mathcal{A} = \mathcal{B} + \mathcal{C}^2/2/\alpha$ and requires a value for α .

	$\tilde{\tau}_c = 1.0$ (\mathcal{C}, \mathcal{B})	$\tilde{\tau}_c = 1.5$ (\mathcal{C}, \mathcal{B})	$\tilde{\tau}_c = 2.0$ (\mathcal{C}, \mathcal{B})
Est. (real space)	(2.27, -2.04)	(2.18, -2.22)	(2.16, -2.23)
inversion error	(0.1, 0.022)	(0.10, 0.14)	(0.11, 0.11)
Est. (redshift space)	(2.25, -2.25)	(2.23, -2.68)	(2.23, -2.68)
inversion error	(0.12, 0.15)	(0.11, 0.12)	(0.12, 0.11)
Est. ($v_{\text{pec}} = 0$)	(2.23, -1.70)	(2.20, -1.81)	(2.19, -1.85)
inversion error	(0.08, 0.25)	(0.08, 0.18)	(0.10, 0.15)
True	(2.27, -1.89)		
cosmic variance	(0.12, 0.16)		

Table 2. The same as the previous table but for mock spectra generated using a skewed PDF with $\mu_3 = 0.4$. Notice that there are two entries for true values in this table. This is because different values of \mathcal{A} are needed to match the observed flux decrement for mock spectra generated with and without peculiar velocities if $\mu_3 \neq 0$.

	$\tilde{\tau}_c = 1.0$ (\mathcal{C}, \mathcal{B})	$\tilde{\tau}_c = 1.5$ (\mathcal{C}, \mathcal{B})	$\tilde{\tau}_c = 2.0$ (\mathcal{C}, \mathcal{B})
Est. (real space)	(2.07, -1.83)	(2.02, -1.95)	(2.00, -1.97)
inversion error	(0.09, 0.18)	(0.10, 0.15)	(0.10, 0.13)
Est. (redshift space)	(2.05, -2.26)	(2.03, -2.29)	(2.03, -2.29)
inversion error	(0.10, 0.16)	(0.11, 0.13)	(0.10, 0.10)
Est. ($v_{\text{pec}} = 0$)	(2.09, -1.95)	(2.07, -2.00)	(2.06, -2.02)
inversion error	(0.08, 0.19)	(0.08, 0.15)	(0.09, 0.13)
True ($v_{\text{pec}} \neq 0$)	(2.08, -1.30)		
cosmic variance	(0.13, 0.19)		
True ($v_{\text{pec}} = 0$)	(2.08, -1.67)		
cosmic variance	(0.13, 0.19)		

Redshift distortions only moderately affect the estimated \mathcal{C} despite substantial differences between the PDFs (see figure 2). The estimates for the three different cutoff values are consistent within the errors, indicating a weak dependence on $\tilde{\tau}_c$.

3.3 Estimated parameters from Q1422

In the top panel of figure 5 we plot the normalized flux of the two spectra of Q1422 obtained independently by Rauch et al. (solid line) and Songaila & Cowie (dotted). There is a good general agreement between the two. As we will see later, the discrepancies caused by the different continuum fits have a moderate effect on the estimated parameters. In the bottom panel of figure 5 we plot the recovered local optical depth in redshift space. The results for both spectra agree very well for $\tilde{\tau} \lesssim 3$. Both curves have a cutoff in saturated regions where the flux goes to zero. The differences at $\tilde{\tau} > 3$ will not affect our estimates of \mathcal{B} and \mathcal{C} because of the truncation at smaller values of $\tilde{\tau}$.

Figure (6) shows $\tilde{\tau}P[\ln(\tilde{\tau})]$ for the recovered $\tilde{\tau}$ from the Rauch et. al. spectrum, in real (solid line) and in redshift space (dashed). The dotted line is for the log-normal with parameters estimated from $\tilde{\tau}$ in real space. There is reasonable agreement between the recovered PDF and the log-normal for low optical depth implying that the true PDF cannot be very different from a log-normal for low densities.

In table (3) we list the estimated values of \mathcal{C} and \mathcal{B} and the value of \mathcal{A} inferred for $\alpha = 1.7$. Because of the strong redshift dependence of \mathcal{A} (eq. 4), we present results from the first half, the second half and the total length of both spectra. We have used a variable Doppler parameter $b = b_0 \tilde{\tau}^{1-\alpha/2}$ with $\alpha = 1.7$. A value of $b_0 = 15\text{km/s}$ matches the χ^2 criterion described in the previous section. As discussed in section 3.2. our inversion procedure works well for cut-off values τ_c up to 2. For $\tau_c = 2$ we

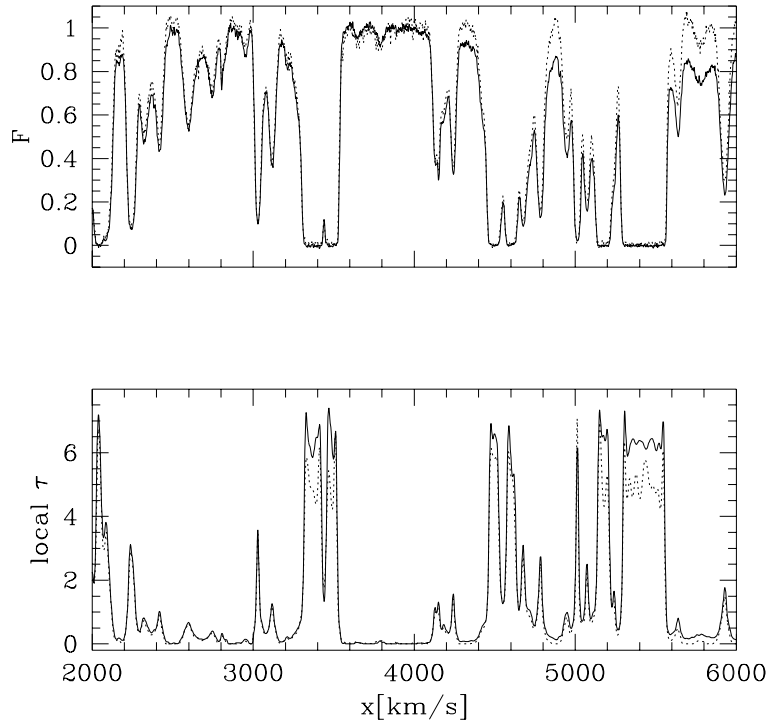


Figure 5. The normalized fluxes (*top*) and recovered local optical depths in redshift space (*bottom*) for a fraction of the two spectra of Q1422. The solid and dotted lines correspond to the spectra observed and continuum fitted by Rauch et. al. and Songaila & Cowie, respectively.

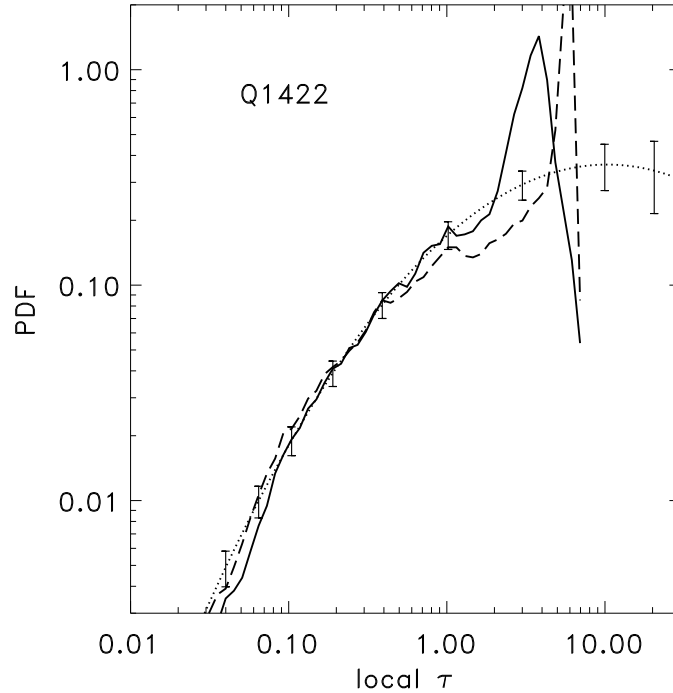


Figure 6. Curves of $\tau P[\ln(\bar{\tau})]$ for the local optical depth in real (solid) and redshift space (dashed) recovered from the Rauch et. al. spectrum. The dotted curve corresponds to the log-normal PDF obtained from the estimated parameters $(C, B) = (1.8, -1.61)$. The error bars are taken from the figure 2.

Table 3. Estimated parameters from the Rauch et al (R) and Songaila & Cowie (SC) observations of the spectrum of q1422+231. Listed are $(\mathcal{C}, \mathcal{B}, \mathcal{A})$ where \mathcal{A} are computed from \mathcal{C} and \mathcal{B} using $\ln(\mathcal{A}) = \mathcal{B} + \mathcal{C}^2/2/\alpha$ and assuming $\alpha = 1.7$. The uncertainty in these parameters is estimated as the maximum total error from the 4 sets of the 70 mock spectra (see text). The absolute 1σ on \mathcal{C} and \mathcal{B} are 0.27 and 0.4.

	$\tilde{\tau}_c = 1.0$ ($\mathcal{C}, \mathcal{B}, \mathcal{A}$)	$\tilde{\tau}_c = 1.5$ ($\mathcal{C}, \mathcal{B}, \mathcal{A}$)	$\tilde{\tau}_c = 2.0$ ($\mathcal{C}, \mathcal{B}, \mathcal{A}$)
Low redshift half			
realspace, R	(1.83,-1.59,0.54)	(1.76,-1.74,0.43)	(1.70,-1.82,0.38)
real space, SC	(2.21,-1.09,1.44)	(2.09,-1.78,0.60)	(2.05,-1.87,0.53)
redshift space, R	(1.82,-1.91,0.39)	(1.79,-1.90,0.38)	(1.71,-1.97,0.32)
redshift space, SC	(2.35,-1.71,0.92)	(2.22,-2.03,0.56)	(2.15,-2.132,.46)
High redshift half			
real space, R	(1.89,-0.89,1.17)	(1.89,-1.32,0.76)	(1.87,-1.35,0.72)
real space, SC	(2.06,-0.63,1.86)	(2.12,-1.26,1.06)	(2.10,-1.34,0.95)
redshift space, R	(1.99,-1.35,0.83)	(1.97,-1.44,0.74)	(1.89,-1.62,0.56)
redshift space, SC	(2.29,-0.95,1.81)	(2.26,-1.55,0.95)	(2.126,-1.84,0.60)
All			
real space, R	(1.89,-1.26,0.81)	(1.84,-1.55,0.57)	(1.80,-1.61,0.51)
real space, SC	(2.14,-0.84,1.66)	(2.13,-1.52,0.83)	(2.09,-1.61,0.72)
redshift space, R	(1.92,-1.66,0.56)	(1.89,-1.70,0.52)	(1.81,-1.82,0.42)
redshift space, SC	(2.35,-1.33,1.34)	(2.26,-1.79,0.75)	(2.14,-1.98,0.53)

obtain $(\mathcal{C}, \mathcal{B}) = (1.8, -1.61)$ and $(\mathcal{C}, \mathcal{B}) = (2.09, -1.61)$ for the Rauch et al and the Songaila & Cowie spectrum, respectively. As discussed in section 3.2. the value of \mathcal{B} is expected to be biased low.

To assign errors to the estimates of \mathcal{C} and \mathcal{B} we draw on the analysis of the mock spectra in the previous section. We take the maximum error of all sets of mock spectra calculated for half the length of the observed spectrum as a conservative error estimate. This gives $\sigma_{\mathcal{C}} = 0.27$. and $\sigma_{\mathcal{B}} = 0.4$, respectively. The values of \mathcal{C} and \mathcal{B} derived from the upper and lower half of the spectrum are consistent within our estimated errors if we account for the expected redshift evolution of \mathcal{B} . The redshift evolution of the clustering amplitude and α and therefore that of \mathcal{C} is expected to be small. The difference between the estimates obtained for the Rauch et al and the Songaila & Cowie spectrum are also consistent within the estimated errors.

For a given value of α we can now infer values of σ and \mathcal{A} from our estimates of \mathcal{C} and \mathcal{B} . The values of \mathcal{A} given in table (3) are derived using

$$\mathcal{A} = \exp[\mathcal{B} + \mathcal{C}^2/2\alpha]. \quad (12)$$

Since \mathcal{B} is systematically biased low, the values of \mathcal{A} in the table should be considered as lower limits. Assuming that the true \mathcal{A} is biased low by a factor of 2 as suggested by our analysis of the mock spectra with $\mu_3 = 0.4$ we estimate $\mathcal{A}(z \approx 3.25) \approx 1.2 \pm 0.7$ ($\sigma_{\ln \mathcal{A}} = \sqrt{(\sigma_{\mathcal{B}}^2 + \sigma_{\mathcal{C}}^2/\alpha)} \approx 0.65$ for $\alpha = 1.7$).

We now discuss the inferred value of $\sigma = \langle \delta^2 \rangle^{1/2}$. For a PDF described by an Edgeworth expansion (equation 11), σ and $\mu_2 = \langle (\log[1 + \delta])^2 \rangle^{1/2}$ are related by

$$\sigma^2 = \left(1 + \mu_2^4 \mu_3 / 3!\right)^{-1} \exp(\mu_2^2) - 1. \quad (13)$$

We have demonstrated in the previous section section that the estimates of \mathcal{C} are unbiased even for true PDFs with rather large skewness parameter μ_3 . The value of $\mu_2 = \mathcal{C}/\alpha$ is therefore also unbiased. Hence by assuming $\mu_3 = 0$ we somewhat overestimate σ . For the values of μ_2 and μ_3 measured in numerical simulations (NH99) we expect this bias to be less than 15%, significantly smaller than the uncertainty in the value of α . We therefore use the relation

$$\sigma^2 = \exp[(\mathcal{C}/\alpha)^2] - 1. \quad (14)$$

Note that the small bias introduced here will also somewhat lower our estimates for Ω in the next section. Possible values of α range between 1.56 and 2 but α is probably about 1.7 at $z \sim 3$ for plausible reionization histories (Hui & Gnedin 1997, Abel & Haehnelt 1999). The estimated value of $\mathcal{C} = 1.8 \pm 0.27$ for the Rauch et al. spectrum translates into $\sigma(\alpha = 2.0) = 1.11 \pm 0.2$, $\sigma(\alpha = 1.7) = 1.44 \pm 0.3$, and $\sigma(\alpha = 1.56) = 1.67 \pm 0.4$. The values for the Songaila & Cowie spectrum are 20 percent higher.

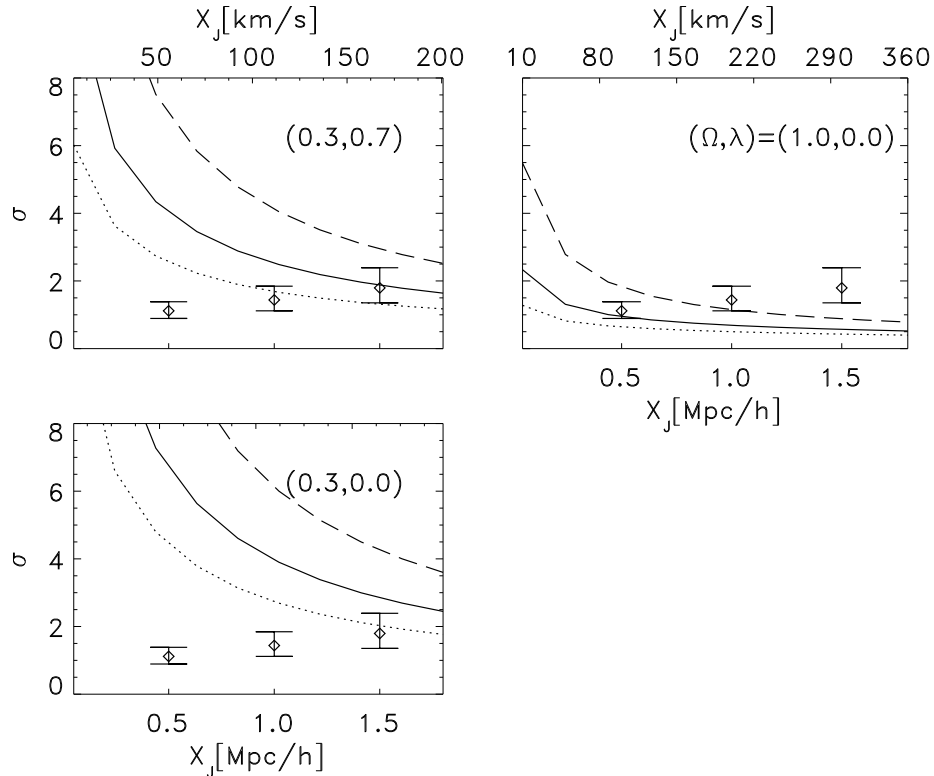


Figure 7. The non-linear rms value of density fluctuations as a function of the effective Jeans length scale. The solid, dotted and dashed curves correspond to $\Gamma = 0.21, 0.1$ and 0.5 , respectively. The three points with error bars are the values estimated from the Rauch et al spectrum of Q1422 for $\alpha = 1.5, 1.7$ and 2.0 (from high to low). The abscissa of the data points are arbitrary and the errors are 1σ and include the error due to cosmic variance and the inversion.

4 COMPARISON WITH THE MASS FLUCTUATIONS AMPLITUDE PREDICTED BY CDM-LIKE COSMOLOGIES: IMPLICATIONS FOR Ω

There is a whole family of CDM-like power spectra which is consistent with a variety of observational constraints on the DM clustering amplitude. If we normalize these power spectra to match the local space density of galaxy clusters (e.g., Eke, Cole & Frenk 1996) then, for a given Ω , we can predict the fluctuation amplitude on the scale and redshift relevant to the estimate of σ in the previous section. In the following we obtain constraints on Ω by comparing our measurement of σ with such model predictions.

We start with the *linear* mass power spectrum as given by Bond, Eftsathiou, Frenk & White (1993)

$$P(k) = \frac{Ak}{[1 + (ak + (bk)^{3/2} + (ck)^2)^\nu]^{2/\nu}}, \quad (15)$$

where the wavenumber k is in units of $1/(h^{-1}\text{Mpc})$, A is a normalizing factor, $a = 6.4\Gamma^{-1}h^{-1}\text{Mpc}$, $b = 3.0\Gamma^{-1}h^{-1}\text{Mpc}$, $c = 1.7\Gamma^{-1}h^{-1}\text{Mpc}$, and $\nu = 1.13$. For standard cold dark matter models the constant Γ is identified with Ωh . The space density of present-day galaxy clusters is reproduced if A is chosen such that the linear rms value, σ_8 , of the density fluctuations in a sphere of radius $8h^{-1}h^{-1}\text{Mpc}$ is given by

$$\sigma_8 = (0.52 \pm 0.04) \Omega^{-0.52+0.13\Omega}, \quad \sigma_8 = (0.52 \pm 0.04) \Omega^{-0.46+0.1\Omega}, \quad (16)$$

for flat and open models, respectively (Eke, Cole & Frenk 1996). We then use an analytic transformation from the linear to the *non-linear* power spectrum (Peacock & Dodds 1996; see also Jain, Mo & White 1995).

In section 2 we introduced an effective Jeans scale x_j such that the fluctuation amplitude of the DM density field smoothed on this scale can be computed from the non-linear power spectrum as

$$\sigma^2(x_j) = \frac{1}{(2\pi)^3} \int_0^\infty dk^3 P_{nl}(k) \left[1 + \left(\frac{kx_j}{2\pi} \right)^2 \right]^{-2}. \quad (17)$$

Even though x_j should be related to the linear Jeans scale, the exact choice of x_j is not obvious and we have left x_j

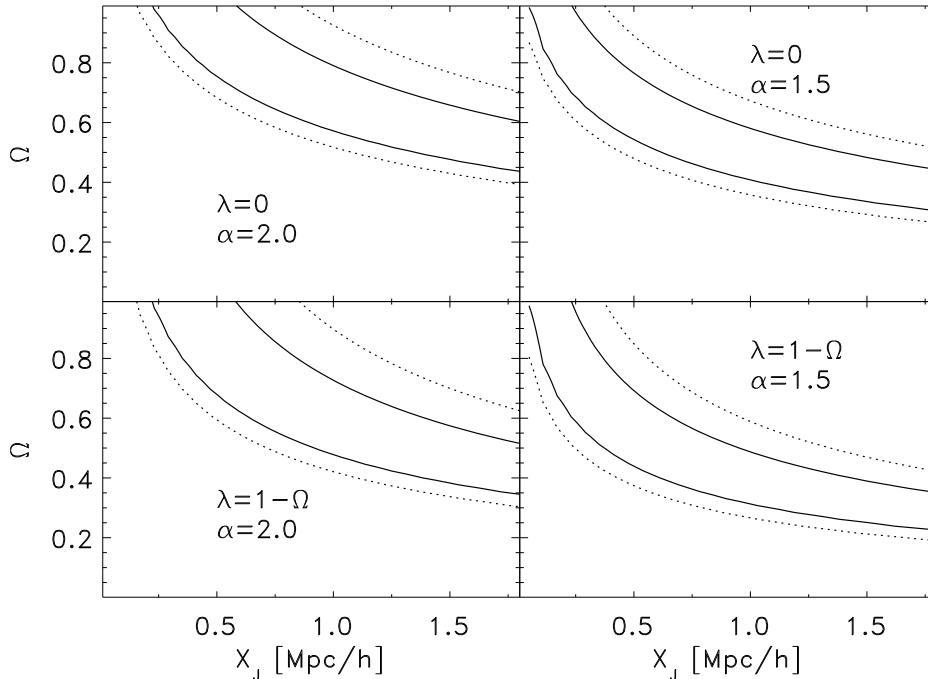


Figure 8. Contours of $\chi^2 = 1$ (solid) and $\chi^2 = 3$ (dotted) as functions of Ω and x_j for two values of α for open and flat models, as indicated in each panel. The χ^2 function quantifies the deviation of the measured clustering amplitude from that predicted by the $\Gamma = 0.21$ model at $z = 3.25$. The error includes cosmic variance, the error due to the inversion and the uncertainty in the normalization of the linear power spectrum.

as a free parameter. The nonlinear σ depends then on the shape parameter Γ , the background density, Ω , the cosmological constant, λ , and the effective Jeans scale, x_j . In figure (7) we show the model prediction for σ at $z = 3.25$ as a function of the effective Jeans scale x_j for different cosmological parameters. The value of σ inferred from the Rauch et al. spectrum is shown as the open symbols with error bars for $\alpha = 1.5, 1.7$ and 2.0 . Three factors contribute to the rather strong Ω dependence of the predicted σ : the power spectrum normalization, the time evolution of the fluctuation amplitude and the relation between length and velocity scale. There is a similar but somewhat weaker dependence on λ .

For a given α , we define the function $\chi^2 = [\mathcal{C}/\alpha - \ln(1 + \sigma^2)/2]^2 / \sigma_{\text{err}}^2$ where the σ_{err} is the total 1σ error including the uncertainty in the power spectrum normalization (16). Figure (8) is a contour plot of χ^2 as function of Ω and x_j for flat ($\Omega + \lambda = 1$) and open models ($\lambda = 0$). If we assume $\Gamma = 0.21$ as inferred from the shape of the power spectrum of the observed galaxy distribution at $z = 0$ (Peacock & Dodds 1994) our estimate for Ω can be expressed in a convenient parametric form as follows: $\Omega = 0.61 (\alpha/1.7)^{1.3} (x_j/0.62)^{-0.6}$ for a flat universe, and $\Omega = 0.91 (\alpha/1.7)^{1.3} (x_j/0.62)^{-0.7}$ for an open universe without a cosmological constant. The errors on Ω are 25%. The inferred values from the Songaila & Cowie spectrum have the same parametric form but are lower by 15%.

5 DISCUSSION

5.1 Comparison to previous work

The value of \mathcal{A}

Rauch et al. have used several HIRES spectra including the one of Q1422+231 used here to infer the value of $\mu = (\Omega_{\text{bar}} h^2 / 0.0125)^2 (H(z) / 100 \text{ km s}^{-1} \text{ Mpc}^{-1})^{-1} (\Gamma_{\text{phot}} / 10^{-12} \text{ s}^{-1})^{-1}$ by comparing the flux decrement distribution of the observed spectra to those of mock spectra calculated from hydrodynamical simulations. This analysis was basically equivalent to a determination of the optical depth constant \mathcal{A} . The two quantities are related as

$$\mathcal{A}(z) \approx 0.71 \mu(z) (\hat{T} / 1.5 \times 10^4 \text{ K})^{-0.7} ((1+z)/4)^6. \quad (18)$$

Rauch et al obtained $\mu(z \approx 3.25) \approx 0.6$ and 1.5 for mock spectra produced from a SCDM model (Hernquist et al. 1996) and Λ CDM model (Cen et al. 1994). The temperatures at $z = 2$ were $\hat{T} = 5.6 \times 10^3$ K and $\hat{T} = 1.1 \times 10^4$ K. This corresponds to $\mathcal{A}(z = 3.25) \sim 1.2$ and 2.0, respectively. No correction for the temperature evolution in the simulations has been made. This is in reasonable agreement with our estimate of $\mathcal{A} \sim 1.2 \pm 0.7$ but we would like to stress that our value includes a rather large correction of a factor two for the bias in \mathcal{B} which we have inferred from our analysis of mock spectra produced with a PDF with $\mu_3 = 0.4$. We therefore do not think that we can currently improve the constraints of Rauch et al. on the baryon density and the flux of ionizing photons. The fact that we obtain a consistent result with a completely different procedure is nevertheless very encouraging. Our value is larger than the $\mathcal{A}(z \approx 3.25) \sim 0.4$ in the fiducial model of Bi & Davidsen ($\alpha = 1.77$).

The value of σ

Gnedin and Hui (1998) used mock spectra calculated from DM simulations to investigate the influence of the fluctuation amplitude on the slope of the column density distribution of QSO absorption lines. They got reasonable agreement with the observed slope if the linear fluctuation amplitude at half the linear Jeans scale for $T = 10^4$ K was about 2. This is larger than our value for the *non-linear* σ . This indicates that the effective Jeans scale is larger than half the linear Jeans scale for $T = 10^4$ K. Bi& Davidsen have assumed $\sigma = 1.95$ in their fiducial model significantly larger than our value $\sigma(\alpha = 1.77) = 1.34$ for the same value of α .

Croft et al. (1998, 1999) have compared the flux power spectrum of observed absorption spectra to infer the DM power spectrum on scales between $2h^{-1}$ Mpc and $12h^{-1}$ Mpc (comoving, $\Omega = 1$) by comparison with mock spectra of DM simulations which were calibrated using hydrodynamical simulations. Note that Croft et al. define their length scales to be a factor 2π larger than we do in our definition of the Jeans length. Croft et al obtain $\Delta = k^3 P(k)/2\pi^2 \approx 0.57 \pm 0.3$ at $z \approx 2.5$, where Δ is the rms fluctuation amplitude of the DM density contributed by a logarithmic interval of k . This measurement was at a scale which corresponds to $x \approx 12(\Omega h^2/0.125)^{-0.5}$ Mpc. Weinberg et al. (1999) then used the constraints on the DM power spectrum obtained by Croft et al. (1999) to constrain the value of Ω with similar assumptions for the normalization and the shape of the power spectrum as we have made here. For $\Gamma = 0.2$ Weinberg et al. 1999 obtain $\Omega \approx 0.34 \pm 0.1$ ($\lambda = 1 - \Omega$) and $\Omega \approx 0.46 \pm 0.1$ ($\lambda = 0$). We obtain somewhat higher values unless the effective Jeans scale is larger than the linear Jeans scale (for a temperature of 15000 K) by about a factor two.

5.2 Future work

There are a number of possible improvements on the analysis presented here. As discussed in section 3.4 the true PDF of the density is expected to be somewhat positively skewed relative to log-normal, but we were not able to constrain the skewness parameter, μ_3 . To make progress on this issue an improved model of the PDF which e.g. relates μ_3 to other parameters would be needed. There are attempts to determine the value of α from the correlation of column density and the lower cut-off of the Doppler parameter distribution (Schaye et al. 1999). Such a determination will obviously improve our constraints on \mathcal{A} and σ . Currently we probe the density PDF up to a rather low overdensity of $\delta \sim 2$. This could be extended to higher densities by incorporating higher order Lyman series line into the inversion scheme. This will tighten the constraints on the density PDF and also extend the redshift range of each spectrum available for the inversion. The main source of uncertainty in our constraints on Ω is the effective Jeans length scale x_j . A calibration of x_j by numerical simulations should help to tighten the constraints on Ω . It should also be possible to extract information on the shape of the power spectrum on small scales from the correlation function of the truncated real-space optical depth. We estimated the error of σ due to cosmic variance to be about 20% for one spectrum like Q1422. This error could be reduced to 5% by applying the method to 20 quasar spectra. Note that the error estimate was based on mock spectra generated with a SCDM power spectrum. It might be different for other power spectra. It would obviously also be interesting to probe the redshift evolution of the clustering amplitude.

6 CONCLUSIONS

We have recovered the real space optical depth distribution along the LOS to the QSO Q1422+231 from two different HIRES spectra of Q1422+231 using the inversion technique proposed by Nusser & Haehnelt (1999). Despite the two spectra having different continuum fits, the difference in the recovered optical depth distribution is small. The recovered optical depth distribution is similar to that expected for a log-normal PDF of the density.

We have used a new technique to estimate the fluctuation amplitude of the gas density and the optical depth constant from the truncated optical depth distribution. Assuming that the PDF of the gas density is log-normal we showed that the moments of the distribution depend on two parameters $\mathcal{B} = \ln[\mathcal{A}/(1 + \sigma)^{\alpha/2}]$ and $\mathcal{C} = \alpha\sqrt{\ln[\sigma^2 + 1]}$. This demonstrates that there are fundamental degeneracies between fluctuation amplitude of the gas, the power law index α , and the optical depth constant \mathcal{A} for a log-normal PDF. These degeneracies will be only very weakly broken if the true PDF is somewhat positively skewed relative to log-normal as expected from numerical simulations.

Using mock spectra we have shown that robust estimates for the parameters \mathcal{B} and \mathcal{C} can be obtained. The mean of the recovered \mathcal{C} is unbiased with respect to the true value. The value of \mathcal{B} however, is systematically biased low if the true PDF is positively skewed relative to log-normal. Our estimates of \mathcal{B} and \mathcal{C} translate into $\mathcal{A} \sim 1.2 \pm 0.7$ and $\sigma \sim 1.44 \pm 0.27$ if we assume $\alpha = 1.7$, the most likely value for plausible reionization histories. The error estimates come from our analysis of the mock spectra. If the IGM indeed traces the DM in the way suggested by simulations this is the first measurement of the fluctuation amplitude on an effective Jeans scale which corresponds to about two hundred kpc(comoving). The fluctuation amplitude of the DM density on such small scales is of particular interest for the question when the epoch of reionization occurs. Our rather low estimate for the value of σ strongly argues for a late epoch of reionization.

Finally, we have compared our measurement of the fluctuation amplitude to predictions by CDM-like cosmogonies with a power spectrum shape parameter suggested by the clustering behavior of galaxies, and normalized to match the observed space density of present-day clusters of galaxies. The fluctuation amplitude of such models depends rather strongly on Ω . We obtain $\Omega = 0.61 (\alpha/1.7)^{1.3} (x_j/0.62)^{-0.6}$ ($\lambda = 1 - \Omega$) and $\Omega = 0.91 (\alpha/1.7)^{1.3} (x_j/0.62)^{-0.7}$ ($\lambda = 0$). If we assume that the effective Jeans scale is close to the linear Jeans scale (at 15000K) then the measured fluctuation amplitude is larger than that predicted for an ($\Omega = 0.3$, $\lambda = 0.7$) Universe by a factor of about two. This argues either for a larger value of Ω and/or a large value of the effective Jeans length x_j .

7 ACKNOWLEDGEMENTS

We are grateful to L. Cowie, M. Rauch, W. Sargent and A. Songaila for letting us use their HIRES spectra of Q1422 for the analysis presented here. We would like to thank T. Theuns and S. White for comments on the manuscript.

REFERENCES

- Adelberger K.L., Steidel C.S., Giavalisco M., Dickinson M.E., Pettini M., Kellog M., 1998, ApJ, in press, astro-ph/9804236
Bahcall J.N., Salpeter E.E 1965, ApJ , 142, 1677
Bahcall N., Fan X. 1998, ApJ, 504, 1
Bechtold J., Crotts A.P.S., Duncan R.S., Fang Y., 1994, ApJ, 437, L83
Bartelmann M., Schneider P., 1999, A&A, 345, 17
Bi H.G., Börner G., Chu Y. 1992, A&A, 266, 1
Bi H.G., 1993, ApJ, 405, 479
Bi H.G., Davidsen A.F., 1997, ApJ, 479, 523
Blanchard, A., Bartlet, J.G. 1998, A&A, 331L, 49
Bond J.R., Szalay A.S., Silk J., 1988, ApJ, 324, 627
Cen R., Miralda-Escudé J., Ostriker J.P., Rauch M., 1994, ApJ, 437, L9
Coles, P., Jones, B.J.T, 1991, MNRAS, 248, 1
Colombi, S., 1994, ApJ, 435, 536
Cooke A.J., Espey B., Carswell R.F., 1997, MNRAS, 284, 552
Couchman H.M.P., Thomas P.A., Pearce F.R., 1995, ApJ, 452, 797
Croft R.A.C., Weinberg D.H., Katz N., Hernquist L., 1998, ApJ, 495, 44
Dinshaw N., Impey, C.D., Foltz C.B., Weymann R.J., Chaffee F.H., 1994, ApJ, 437, L87
Ecke, V.R., Cole, S., Frenk, C.S., 1996, MNRAS, 282, 263
Fisher K.B., Lahav O., Hoffman Y., Lynden-Bell D., Zaroubi S., 1995, MNRAS, 272, 885
Gaztanaga E., Croft R.A.C., 1998, astro-ph/9811480
Gnedin N., Hui L., 1998, MNRAS, 296, 44
Gunn J.E., Peterson B.A., 1965, ApJ, 142, 1633
Haehnelt M., Steinmetz M., 1998, MNRAS, 298, L21
Hernquist L., Katz N., Weinberg D.H., Miralda-Escudé J., 1996, ApJ, 457, L51
Hui L., Gnedin N.Y., 1997, MNRAS, 292, 27
Hoffman, Y., Ribak, E., 1991, ApJ, 380L, 5
Jain, M., Mo, H., White, S.D.M., 1995, MNRAS, 276, L25
Jenkins A., Frenk, C.S., Pearce, F.R., Thomas, P.A., Colberg, J.M., S.D.M., Couchman, H.M.P., Peacock, J.A., Efstathiou, G., Nelson, A.H., 1998, ApJ, 499, 20
ofman L., Bertschinger E., Gelb, J., Nusser A., Dekel A., 1994, ApJ, 420, 44.
Lucy L. B., 1974, *Astronomical. J.* 79, 745
MacFarland T.J., Couchman H.M.P., Pearce F.R., Pichlmeier J., 1998, astro-ph/9805096
McGill C., 1990, MNRAS, 242, 544
Miralda-Escudé J., Cen R., Ostriker J.P., Rauch M., 1996, ApJ, 471, 582
Nusser A., Dekel A., Bertschinger E., Blumenthal G., 1991, *Astrophys. J.* 379 6
Nusser A., Haehnelt M., 1991, MNRAS, 303, 179
Peacock J.A., Dodds S.J., 1994, MNRAS, 267, 1020
Peacock J.A., Dodds S.J., 1996, MNRAS, 280, L19

- Petitjean P., Mucket J.P., Kates R.E., 1995, *A&A*, 295, L9
- Petitjean P., 1997, in: *The Early Universe with the VLT*, ed. Bergeron J., ESO Workshop, Springer, p.266
- Press W.H., Teukolsky S.A., Vetterling W.T., Flannery B.P., *Numerical Recipes*, 1992, second edition, Cambridge University Press.
- Rauch M., Miralda-Escudé J., Sargent W.L.W., Barlow T.A., Weinberg D.H., Hernquist H., Katz N., Cen R., Ostriker J.P. 1997, *ApJ*, 489, 7
- Rauch M., 1998, *ARAA*, in press
- Schneider D.P., Schmidt M., Gunn J.E., 1991, *AJ*, 101, 2004
- Sheth R., 1998, *MNRAS*, 300, 1057
- Sigad Y., Eldar A., Dekel A., Strauss M.A., Yahil A., 1998, *ApJ*, 495, 516
- Songaila A., Cowie L.L., 1996, *AJ*, 112, 335
- Theuns T., Leonard A., Schaye J., Efstathiou G., Pearce F.R., Thomas P.A., 1998, *MNRAS*, 301, 478
- Wechsler, R.H., Gross, M.A.K., Primack, J.R., Blumenthal, G.R., Dekel, A., 1998, *ApJ*, in press, astro-ph/9712141
- Weinberg D.H., 1992, *MNRAS*, 254, 315
- Weinberg D.H., Miralda-Escudé J., Hernquist L., Katz, N., 1997, *ApJ*, 490, 564
- Weinberg D.H., Miralda-Escudé J., Hernquist L., Katz N., Miralda-Escudé J., 1998, in: *Structure and Evolution of the IGM from QSO absorption lines*, eds. Petitjean P., Charlot S., Editions Frontieres, p. 133
- Weinberg D.H., 1999, in: *From Recombination to Garching*, eds. Banday T. et al.
- Weinberg D.H., Croft R.A.C., Hernquist L., Katz N., Pettini M., 1999, *ApJ*, submitted
- Wiener, N. 1994, in *Extrapolation and Smoothing of Stationary Time Series*, (New York, Wiley)
- Yahil, A., Strauss, M.A., Davis, M., Huchra, J.P., 1991, *ApJ*, 372, 380
- Zaroubi S., Hoffman Y., Fisher K.B., Lahav O., 1995, *ApJ*, 449, 446
- Zhang Y., Anninos P., Norman M.L., 1995, *ApJ*, 453, L57

